26th EPS Conf. on Contr. Fusion and Plasma Physics, Maastricht, 14 - 18 June 1999 ECA Vol.23J (1999) 1597 - 1600

Simulation of Stochastic (E×B) Diffusion of Ions in a Spatially Periodical Potential Field

M. Tendler[1],L. Krlín, J.Stöckel, V. Svoboda[2]

Institute of Plasma Physics, Czech Acad. Sci., P.O. Box 17, 182 21 Prague 8, CZ
[1]*Alfven Laboratory, Royal Institute of Technology, 10044 Stockholm, Sweden*
[2]*Fac. of Nuclear Sciences and Physical Engineering, Czech Tech. Univ., Prague 1, CZ*

Low-frequency turbulence in a tokamak plasma results in a creation of potential structures in an edge tokamak plasma. It is supposed that these structures cause an anomalous ion diffusion from the tokamak.

There exist several models, which enable to find possible mechanisms of the diffusion and to estimate diffusion coefficients. Our model, under the description, consists in the modelling of the potential structure by means of a spatially periodical and time independent structure. Considering further a homogeneous magnetic field (corresponding to the tokamak magnetic field), it is possible to follow trajectories of individual particles by means of direct numerical integration of corresponding equations of motion. From this simulation follows that particles are trapped either in these structures, or perform rather random motion in the potential landscape [1]. The chaotic dynamics is given by the non-integrability of corresponding Hamiltonian. This therefore generalizes the approach of Bellan [2]. We choose a simple spatial periodicity of the potential as $U = U_0(2 + \cos kx + \cos ky)$. The wavenumber k defines the spatial periodicity in the $x - y$ plane. This potential is plotted in Fig. 1 (axonometric view) and Fig. 2 (equipotential lines) in dimensionless coordinates $\xi = kx, \quad \eta = ky$. The potential landscape is a periodic mesh of maxima (hills) and minima (valleys) of potential. The distance between adjacent hills (or valleys) is $\lambda = 2\pi/k$. The equipotential lines with $U/U_0 = 2$ divide the potential landscape into rectangular cells, each containing either an individual hill or a valley and they form the *separatrices*. The cross-points between the separatrices, chacterized by $E_x = E_y = 0$ are the X - *points*.

The trajectory of a test ion in such potential and magnetic field is described by the equation

$$m\frac{\mathrm{d}\mathbf{v}}{\mathrm{d}t} = q(\mathbf{E} + \mathbf{v} \times \mathbf{B}); \quad \mathbf{E} = -grad\, U; \quad \mathbf{B} = (0, 0, B_z). \tag{1}$$

Here, $m = Am_p$ and $q = Z|e|$ is the mass and the charge of the test ion (A, Z being the mass and charge numbers, respectively), $\mathbf{v}$ is its velocity vector, and $\mathbf{E}$ and $\mathbf{B}$ are the vectors of the electric and magnetic field, respectively.

Using the dimensionless system $\xi = kx, \quad \eta = ky, \quad \theta = \frac{Zq_pB}{Am_p}\, t = \omega_c\, t$, ($|e| = q_p$, ω_c is the ion cyclotron frequency), the equations of motion take the form

$$\frac{\mathrm{d}^2\xi}{\mathrm{d}\theta^2} = R\sin\xi + \frac{\mathrm{d}\eta}{\mathrm{d}\theta}; \quad \frac{\mathrm{d}^2\eta}{\mathrm{d}\theta^2} = R\sin\eta - \frac{\mathrm{d}\xi}{\mathrm{d}\theta}. \tag{2}$$

where $R = \frac{Am_pU_0k^2}{Zq_pB_z^2}$ is the dimensionless parameter governing ion motion.

Using the dimensionless coordinate system, we have shown that the dynamics is completely determined by two parameters, namely, by the parameter R, and by the dimensionless velocity $\nu = (k/\omega_c)v_0$, where v_0 is the initial velocity of the particle.

Very recently [1], we have discussed the most simple case, $R \neq 0$, $\nu = 0$.

We followed trajectories of 1000 test particles, choosing the dimensionless ratio R as a parameter. These particles are randomly launched from the area, situated in both adjacent regions around the separatrix and defined by a square in Fig. 2. Their initial velocities are again considered to be zero.

The trajectory of each particle is monitored during a sufficiently long time interval θ_f corresponding to ~ 50 circumnavigations around a hill or valley.

The squared displacement of the jth particle from the starting position $(\xi_j(0), \eta_j(0))$, $\Big(\Delta\rho_j(\theta)\Big)^2 = \Big(\xi_j(\theta) - \xi_j(0)\Big)^2 + \Big(\eta_j(\theta) - \eta_j(0)\Big)^2$ is registered with a time step $\Delta\Theta = \theta_f/20$.

Then, the variance of the displacement is calculated as $< (\Delta\rho)^2 >= \frac{1}{N}\sum_{j=1}^{N} \Delta\rho_j^2$. The normalized diffusion coefficient D_n is determined in this case from the θ derivative of the variance $< (\Delta\rho)^2 >$ as $D_n = \frac{1}{4}\frac{\mathrm{d}}{\mathrm{d}\theta} < (\Delta\rho)^2 >$.

From the numerical simulation follow three regimes of the particle dynamics. For low values of R, the particles are trapped in the potential structures, drifting along equipotential lines. For larger values of R, particles start to diffuse among the potential structures, and the diffusion has a brownian motion character. For yet larger values of R, due to the strong non-linearity of the problem, the strange character of trajectories can be identified with the dynamics, usually described as *Lévy-walks* [3]. This dynamics consists in the intermittency of the travelling over the potential landscape without trapping, following by sudden trapping etc.

The diffusion of heavier ions (represented by impurities like carbon) can be rather fast. The diffusion of bulk plasma ions is negligible, even for large thermal velocities. Due to this fact, our model, based on test particle approximation, is adequate.

Since the present model is interesting not only from the point of theory, but also for possible applications, we have discussed it more properly.

First we have studied two-parametric model, with $R \neq 0, \nu \neq 0$, expecting fundamental diferences from the case $\nu = 0$, and, possibly, the non-negligible diffusion of plasma ions. Nevertheless, the differences are not dramatical. This is seen in Fig. 3., where the dimensionless difusion coefficient is presented for $\nu = 0$, $\nu = 2$ and $\nu = 4$. The region $R \leq 1$, which corresponds to experimentally detected amplitudes of the potential, is changed only slightly. On the contrary, the case $\nu \neq 0$ enables the diffusion of particles, originally situated in potential valleys (for the case $\nu = 0$, valleys's particles were unifluenced by the diffusion at all [1], see Fig. 5). This presents Fig. 4, where from the original amount of one thousand of particles, randomly situated in the potential landscape, more than 500 particles start to diffuse (and, therefore, also valleys's particles).

Further, to obtain more informations on the complicated dynamics, we started to study the velocity power spectrum of trajectories. Three different modes of particles's behaviour, mentioned above are presented in Figs. 5-7 together with theirs corresponding power spectrum. The difference between random-walk-like dynamics and Lévy walks, expressed by their correlation functions, is remarkable.

Finally, there appeared one interesting application of our model. *M. Tendler* proposed to use it for the possible generation of radial electric fields on rational surfaces of tokamaks. It is well known that in the neighbourhood of these surfaces, low-frequency turbulence appears, with concomitantly appearing electrostatic potential. This has simi-

lar properties as our model of potential. Since the diffusion of impurities is rather fast (as we have found), expelling these ions from this layer can create radial electric field, and, consequently, the shear rotation of plasma. This effect can contribute to the formation of the transport bariers.

[1] Krlín L., Stöckel J., Svoboda V. 1999 *Plasma Phys. Control. Fusion* **41** 339.
[2] Bellan P.M. 1991 *Plasma Phys. Control. Fusion* **35** 169
[3] Klafter J. et al. 1996 *Phys. Today* **2** 33.

Figures

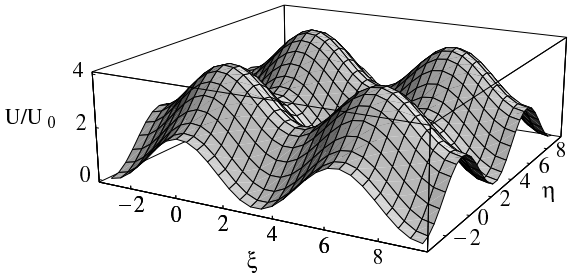

Fig. 1. Potential landscape (axonometric view).

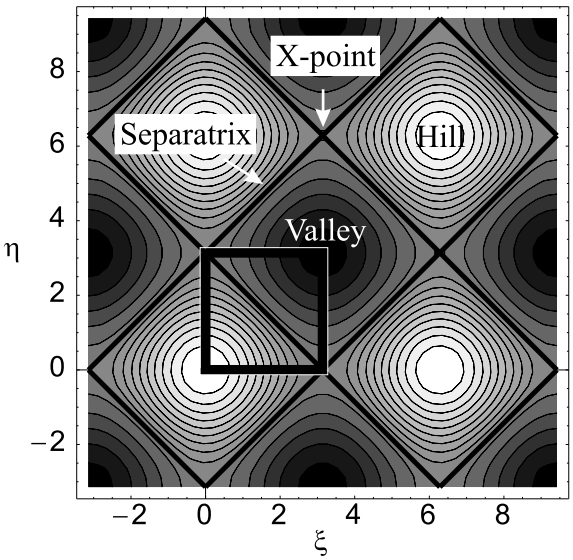

Fig. 2. Equipotential lines for hills and valleys separated by separatrices.

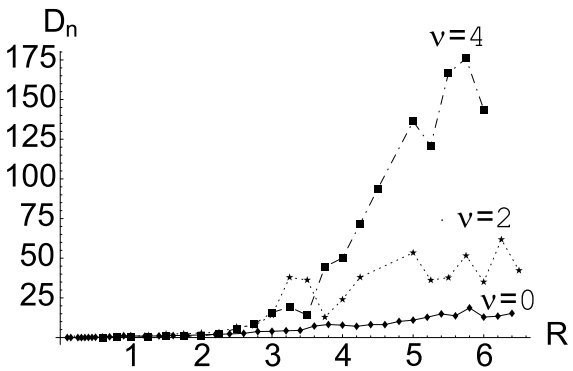

Fig. 3. Normalized statistical diffusion coefficient D_n as a function of R.

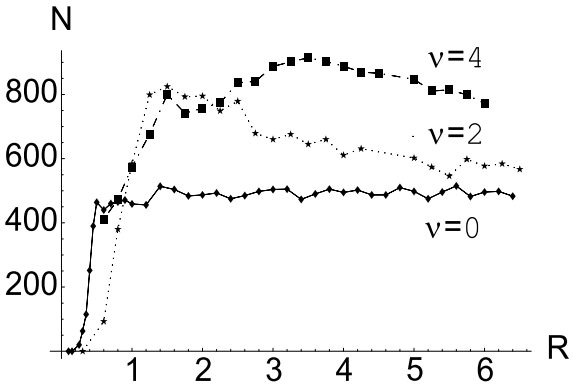

Fig. 4. Number N of test particles (from 1000 particles investigated), escaping from the investigated area (see Fig. 2) after the period θ_f, as a function of R

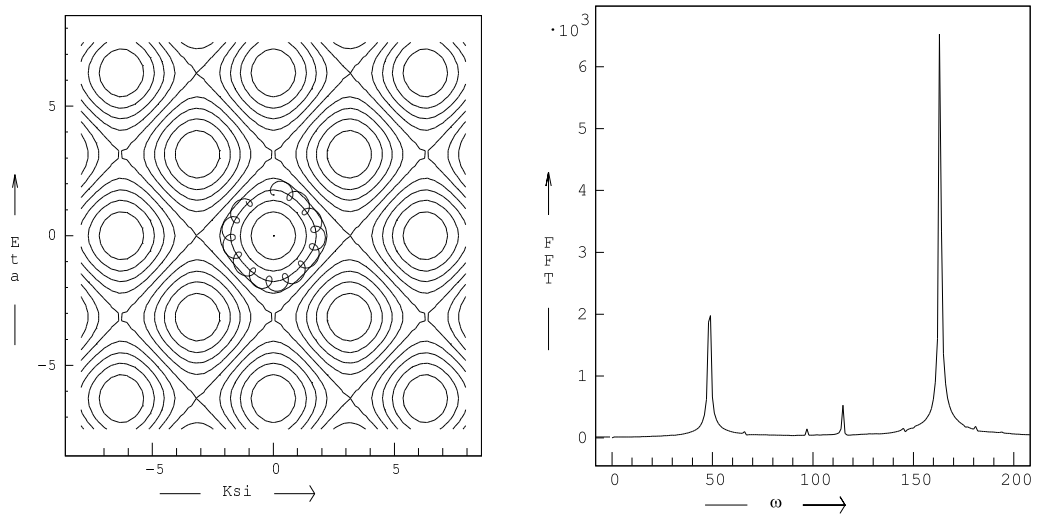

Fig. 5. Regular motion of an ion situated initially to the potential hill and its power spectrum.

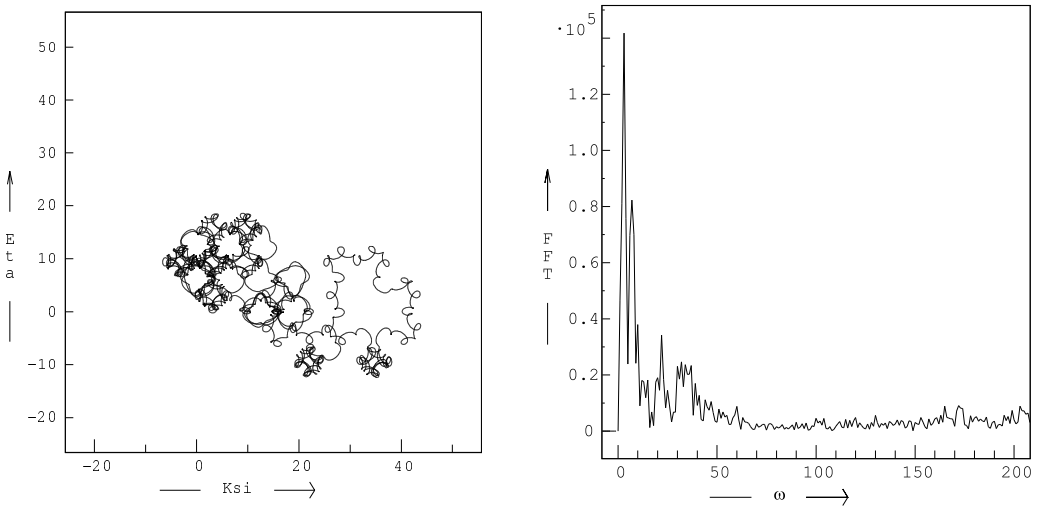

Fig. 6. Stochastic trajectory of a test ion and its power spectrum; example of the random walk.

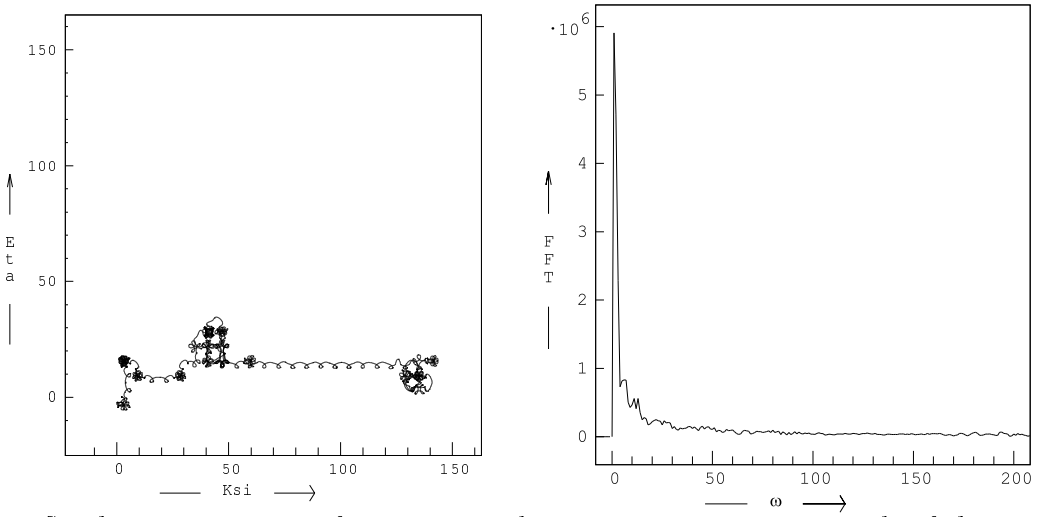

Fig. 7. Stochastic trajectory of a test ion and its power spectrum; example of the Lévy walk.